

ARTICLE

Received 15 Feb 2016 | Accepted 8 Feb 2017 | Published 27 Mar 2017

DOI: 10.1038/ncomms14884

OPEN

A coupled human-Earth model perspective on long-term trends in the global marine fishery

E.D. Galbraith^{1,2,3}, D.A. Carozza^{3,4} & D. Bianchi⁵

The global wild marine fish harvest increased fourfold between 1950 and a peak value near the end of the 20th century, reflecting interactions between anthropogenic and ecological forces. Here, we examine these interactions in a bio-energetically constrained, spatially and temporally resolved model of global fisheries. We conduct historical hindcasts with the model, which suggest that technological progress can explain most of the 20th century increase of fish harvest. In contrast, projections extending this rate of technological progress into the future under open access suggest a long-term decrease in harvest due to over-fishing. Climate change is predicted to gradually decrease the global fish production capacity, though our model suggests that this is of secondary importance to social and economic factors. Our study represents a novel way to integrate human-ecological interactions within a single model framework for long-term simulations.

¹Institució Catalana de Recerca i Estudis Avançats (ICREA), Pg. Lluís Companys 23, Barcelona 08010, Spain. ²Department of Mathematics, Institut de Ciència i Tecnologia Ambientals (ICTA), Universitat Autònoma de Barcelona, Barcelona 08193, Spain. ³Department of Earth and Planetary Sciences, McGill University, Montreal, Québec H3A 0E8, Canada. ⁴Department of Mathematics, Université du Québec à Montréal, Montréal, Québec H3C 3P8, Canada. ⁵Department of Atmospheric and Oceanic Sciences, University of California, Los Angeles, California 90095, USA. Correspondence and requests for materials should be addressed to E.D.G. (email: eric.galbraith@uab.cat).

The global capture of wild marine ‘fish’ (including edible invertebrates, as well as true fish) appears to have peaked in the 1990s, according to a recent reconstruction¹ (Fig. 1a), despite continued increases in the effort expended by the global fishery² (Fig. 1b). The increasingly intense fishing pressure has driven marine fish biomass to a fraction of its pristine state (Fig. 1c), a depletion that is widely believed to be limiting fishing yields in many parts of the world^{2–4}. These historical trends reflect the interplay of ecosystem dynamics, the demand for fish, the cost of fishing, improvements of fishing technology and climate change^{1,3,5–7}, all of which will play a role in future^{8–10}, but whose relative roles have been difficult to formally assess.

Here we quantitatively address the multiple influences in the global fishery, and their interactions, by explicitly including human activity within an Earth System modelling framework, and using simulation protocols typically used for climate simulations. We use the BiOeconomic mARine Trophic Size-spectrum (BOATS) model, a bio-energetically constrained macroecological-life-history fish model that is coupled directly with an economic model^{11,12} (Methods, see Supplementary Methods for details). The BOATS model builds on prior works that took regional¹³, species-specific or unidirectional coupling approaches^{14,15} by introducing a comprehensive two-way coupling of human and natural components of the system, using relatively simple but well-founded predictive principles applicable to multi-decadal timescales. Primary production by phytoplankton and seawater temperatures are used to predict the growth and reproduction of fish, by determining the energy available to the trophic web¹⁶ and the metabolic rates of size-structured fish populations¹⁷. The fish harvest is determined by local-biomass density and interactive fishing effort, which evolves independently in each grid cell over time. As a first-order approximation, we assume that individual fishermen are rational and profit-seeking, as generally borne-out by observations¹⁸, and that there are no property rights (Open Access (OA)), which is the expected outcome in unmanaged fisheries. The current model version does not simulate artisanal or recreational fisheries explicitly, but only industrial fisheries, which account for >80% of global harvest and most of the 20th century trend¹. Although the OA dynamic is not representative of the ~40% of fisheries where management has recently become relatively effective¹⁹, it was a reasonable approximation of global fisheries throughout most of the 20th century²⁰ and remains reflective of at least half of fisheries today, particularly in low-income countries^{21,22}. Poorly constrained ecological model parameters are calibrated using Monte Carlo-based approximate Bayesian computation (Methods, Supplementary Methods) by comparing simulated with observed catch and biomass, aggregated at the scale of Large Marine Ecosystems (LMEs). The use of globally distributed LMEs allows the assessment of model performance across the full range of extant environmental conditions¹². We show results for an ensemble of five different combinations of parameter values that provide realistic solutions, while representing a broad range of parameter uncertainty.

Because the model resolves the dynamics of the global fishery as a function of economic and environmental conditions, historical ‘hindcast’ simulations can be conducted to attribute the historical harvest trend to possible drivers on the coupled system, analogous to the approach taken with coupled ocean-atmosphere models to identify the role of greenhouse gases in historical climate²³. Given our simple but inclusive conceptual framework, the external factors influencing the long-term development of the wild capture fishery are climate, the price of fish, the cost of fishing and the technology-dependent ability of fishermen to catch fish for a given amount of fishing effort. We

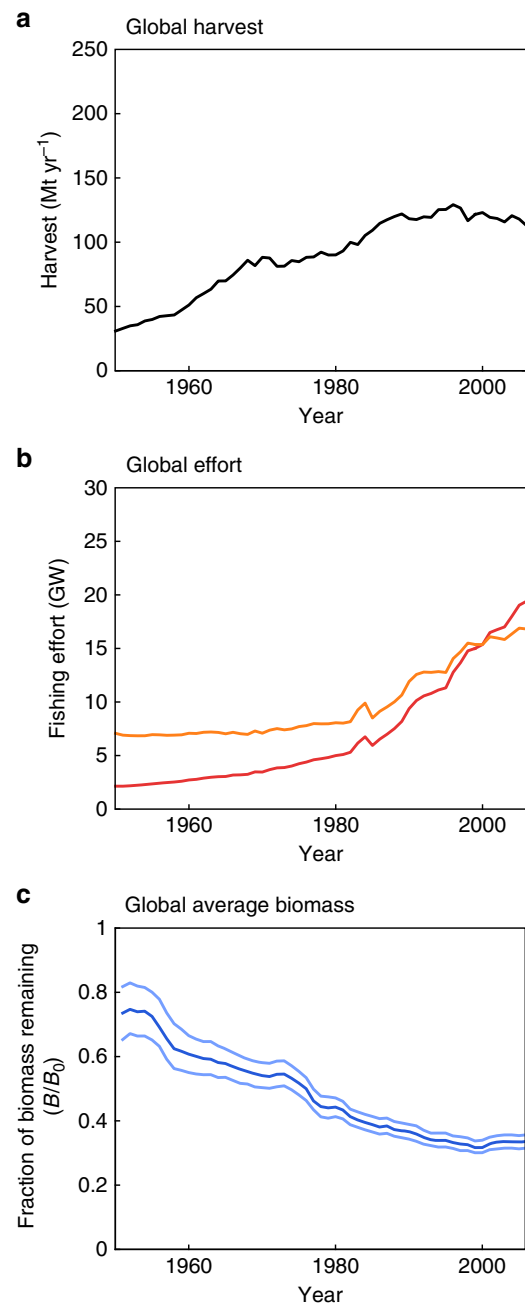


Figure 1 | Global historical time-series characterizing the global wild capture fishery. (a) Reconstructed global fish harvest¹, including illegal, unreported and underreported catches. (b) Estimated nominal effort (orange) and effective effort assuming, conservatively, an increase in efficiency of 2.4% per year (red) (ref. 2). (c) Biomass as a fraction of pristine biomass from selected stock assessment data, as estimated by ref. 4.

first consider the ability of these factors to explain broad features of the observed 20th century trend of fish harvests, and then consider their possible roles in the future of the wild capture fishery.

Our results show that the historical increase of wild fish harvest, aggregated at the global scale, can be reproduced to first order by a hindcast that includes a moderate rate of increase in the technology-dependent ability to catch fish over time, assuming open access. We also show that, were it to continue, this same rate of technological progress would dominate the

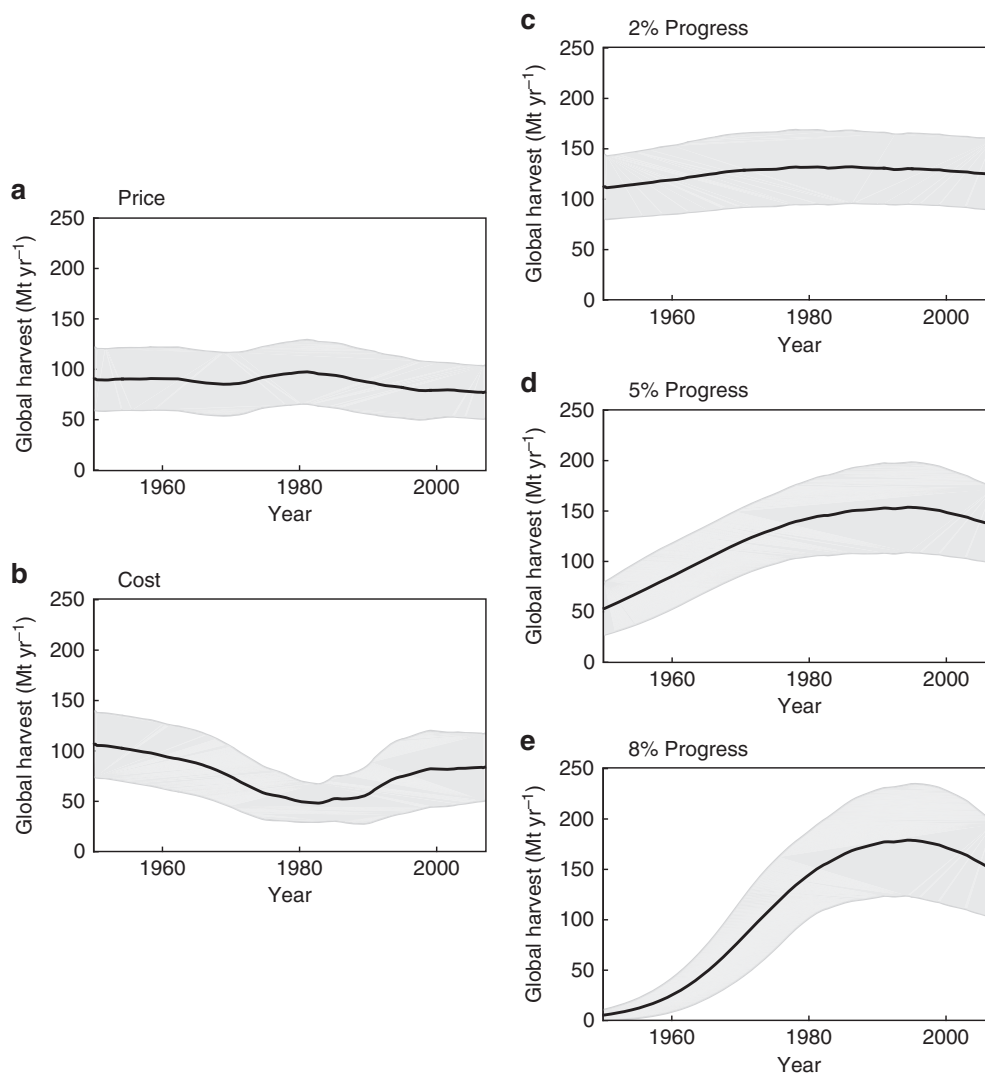


Figure 2 | Attribution of drivers using model hindcasts of the global fishery. All simulations assume OA, and each varies only the forcing specified; all other ecosystem and economic dynamics are solved prognostically. The average ex-vessel price of fish (a) and cost of fishing per unit effort (b) are derived from observations, while technological progress is imposed as a constant rate of catchability increase of (c) 2, (d) 5 and (e) 8% per year.

future trend in fish harvest under open access, but would result in declining, rather than increasing, harvest. The future simulations also assess the relative impacts of climate change on fish harvest, with and without effective management of fisheries, and considering the possibility of increasing market demand.

Results

Hindcast simulations. We carried out a series of experiments in which the model was subjected to temporally varying histories of the three economic forcings: (1) ex-vessel fish price (that is, the price that fishermen receive per mass of catch), which has varied over time in response to market conditions; (2) cost per unit effort, which includes capital, fuel, labour and the impact of most subsidies and (3) technological progress (Supplementary Methods). Our definition of technological progress includes advances in embodied technology, including more efficient boats, more effective fishing gear, sonar and communications equipment and disembodied technology, such as better knowledge of fish behaviour and more efficient fishing practices²⁴. The combined effect of embodied and disembodied technology is represented in a simple but inclusive way by a catchability parameter, which was increased at rates of 2, 5 and 8% per year, a

range representative of progress estimated empirically from individual fisheries^{7,25–27}.

As shown in Fig. 2, the simulated changes in global harvest do not reproduce the observed increasing 20th century trend when forced individually with reconstructed changes in price or cost alone. Given the open-access assumption, this implies that increasing demand for fish was not the main driver of the long-term 20th century increase in fish harvest, despite population growth, although a growing population may have helped to maintain demand in the face of an increasing fish supply. Nor could the reconstructed changes in the cost per unit effort of fishing have been the primary driver. In contrast, the three simulations with technical progress produce global histories of harvest with long-term 20th-century increases, more consistent with the observations. With increasing technology the model also simulates a global peak of harvest, as observed, which arises from the sequential development, overexploitation and/or collapse of fisheries throughout the world, a sequence that has occurred historically in poorly managed fisheries^{28,29} (Supplementary Methods).

The technological progress rate of 5% per year would appear most representative as a global, long-term average, given that it

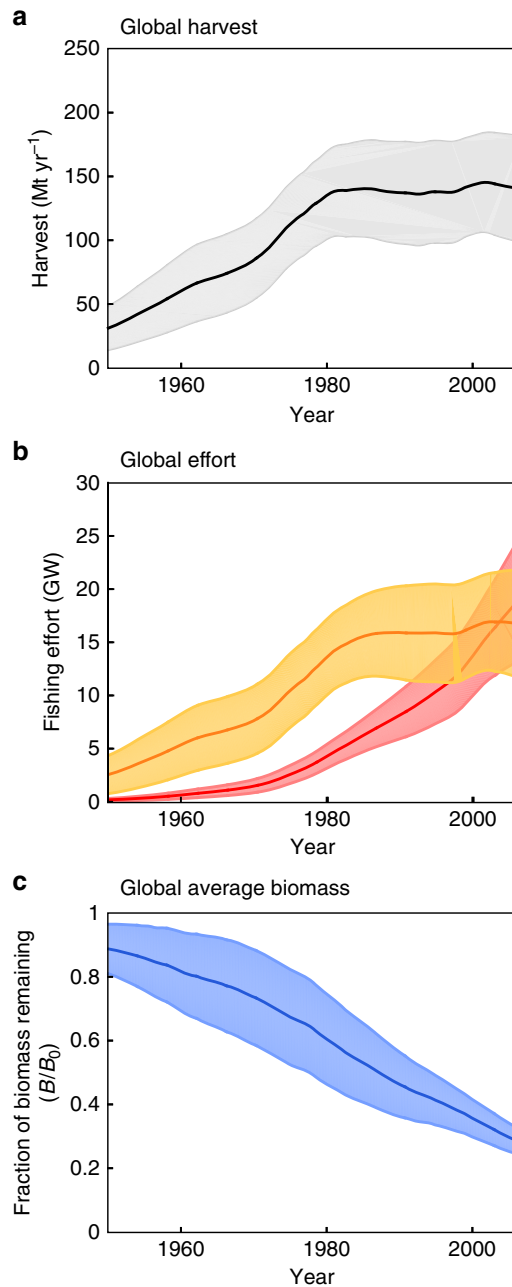


Figure 3 | Global historical hindcast simulation. Lines and shaded areas show the model ensemble mean and 1 s.d., respectively, assuming open access (OA, that is, no regulation), 5% per year technological progress, the observed history of ex-vessel price, and historical climate variability as simulated by the IPSL climate model. **(a)** Simulated fish catch per year. **(b)** Nominal effort (orange) and effective effort (red). **(c)** Simulated biomass as a fraction of pristine biomass. All model forcings and parameters other than technology, price and climate are held constant throughout the 56-year simulation.

approximates the observed relative increase of harvest between 1950 and 1996 and is near the midpoint of estimates from individual fisheries^{7,27,30}. Given this apparent support for a long-term average technological progress rate of roughly 5% per year, we apply it together with the historical price reconstruction to generate a standard global hindcast, shown in Fig. 3. The agreement of the hindcast simulation with the reconstructed fish harvest, effort and biomass (compare Fig. 3 with Fig. 1) is remarkable, given that these are emergent properties of the

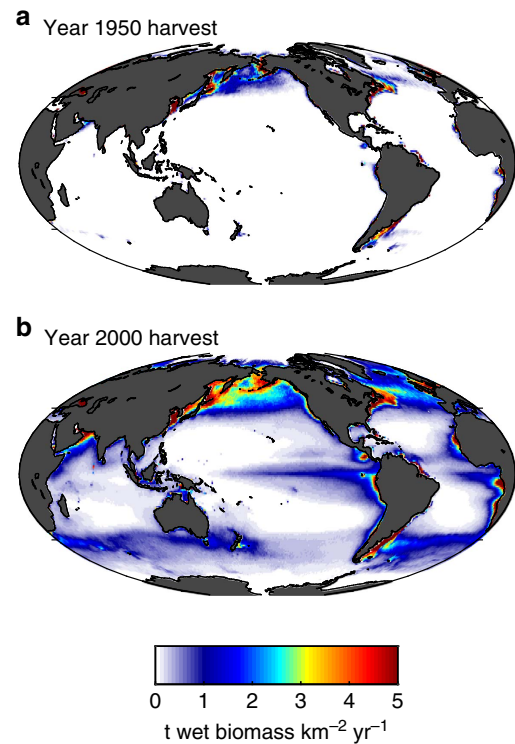


Figure 4 | Spatial expansion of fisheries in historical hindcast simulation.

Ensemble-average harvest in years 1950 **(a)** and 2000 **(b)**. Colour shading shows the harvest in t km⁻² yr⁻¹. For these plots, the ensemble was forced with satellite-based observational estimates of primary productivity and temperature, subjected to globally homogeneous historical price variations and steady 5% per year technological progress. Although idealized, the simulations reproduce key aspects of late 20th century changes, including a shift to lower latitudes and deeper waters.

model. The effort estimated before 1970 (~7 GW) is notably higher than that simulated by the model ensemble (1–5 GW), but given difficulties in reconstructing historical global fishing effort², these contrasts may not be significant. The estimated rate of biomass decrease is well-reproduced by the model at ~10% of pristine biomass per decade, but with an important difference following 1990 when the estimated rate of biomass loss slowed (Fig. 1c), in contrast with the model. This divergence would be consistent with a progressive improvement in the management of many fisheries over the past three decades, a change that is not captured by the idealized OA simulations.

The model simulations also reproduce the first-order aspects of the 20th-century spatial changes in fish harvest, first depleting the dense biomass of highly productive coastal waters³¹, and then moving into deeper waters of the open ocean^{32,33} (Fig. 4). The expansion away from the coasts arises in the model as technological progress makes open-ocean waters with low biomass density more profitable, and therefore increasingly subjected to fishing effort. It should be emphasized that this model does not account for higher costs of fishing far from port, nor does it include complex ecosystem interactions, habitat alteration, fisheries management, or spatially variable economic factors, all of which played some role in the history of the global fishery. Nonetheless, it successfully reproduces the first-order features of the historical global trends in harvest, and biomass. We therefore hypothesize that technological progress, at an average rate of ~5% per year, dominated the development of the global wild capture fishery during the 20th century, while other societal, economic and climate forces had secondary impacts.

Idealized future projections. We consider an extreme range of possible futures for the global wild-capture fishery by projecting the model forward under idealized economic scenarios, with and without climate change. First, the historical OA hindcast is projected forward to represent an extreme end-member in which management is absent, under two alternative technological progress scenarios, and with either constant or linearly increasing price (Methods). Second, the model is used to estimate the global Maximum Sustainable Yield (MSY), representing the theoretical upper limit that could be approached with perfectly effective and well-informed management aimed at maximizing food production (Supplementary Methods). We emphasize that the future of the global fishery will follow neither the purely OA nor the MSY pathway; rather, these end-members outline the boundaries of what is possible for the global wild fishery in terms of food production. For example, effective regulations aimed at maximizing economic yield would produce less than the MSY harvest, but would generate more profit for fishermen¹⁹. We simultaneously consider the impacts of climate change by using water temperatures and primary production from the Institut Pierre Simon Laplace (IPSL) Earth System model with the RCP8.5 scenario (high emissions), and compare with a stable pre-industrial climate (Methods, Supplementary Methods).

The MSY is determined exclusively by the ability of the ecosystem to produce harvestable biomass, so that this modelled upper limit of potential harvest depends only on climate. As shown by Fig. 5a, the model ensemble estimates a MSY of $\sim 180 \pm 60 \text{ Mt yr}^{-1}$ under stable preindustrial climate, while the inclusion of historical climate change leads to a decrease of MSY to $160 \pm 50 \text{ Mt yr}^{-1}$ by 2015. The present-day global MSY estimate of 123 Mt yr^{-1} provided by ref. 19 lies within the 1 s.d. range of the model ensemble. Under the rapid continuing climate change of the RCP8.5 scenario, MSY decreases by 20% relative to 2015 by the end of the 21st century, falling below the simulated peak harvest obtained under OA, consistent with the view that climate change will cause a significant drop in potential fish production without reduction of carbon emissions³⁴.

However, a much more dramatic decline in global harvest occurs over the 21st century in the hypothetical cases for which effective management is absent, as illustrated by the OA scenarios. Given continued 5% per year technological progress and constant price, the peak in global harvest is followed by a long-term decline (Fig. 5a, grey). This reversal in the role of technological progress—from enhancing to reducing harvest—arises because the ability of most ecosystems to produce biomass becomes limited by the spawning stock size under intense rates of harvest, as shown in many scientific surveys of fisheries^{35,36}, and constrained here through our calibration against observed harvests (Methods, Supplementary Methods). If technological progress is halted, the harvest stabilizes, with only a small downward drift that is due to climate change (Fig. 5a, green). In the OA simulations where future price increases, shown in Fig. 5b, the same general trajectories are maintained, but the decline of harvest is more severe because over-fishing is intensified.

Discussion

Our hindcast simulations, forced with relatively simple historical scenarios, suggest that a long-term average technological progress rate of roughly 5% per year dominated the 20th century trend in global fish harvests. In reality, technological improvements did not proceed by a steady march synchronized throughout the world, but proceeded at heterogeneous rates among different fisheries according to the development and diffusion of new ideas, and access to the capital required to implement them.

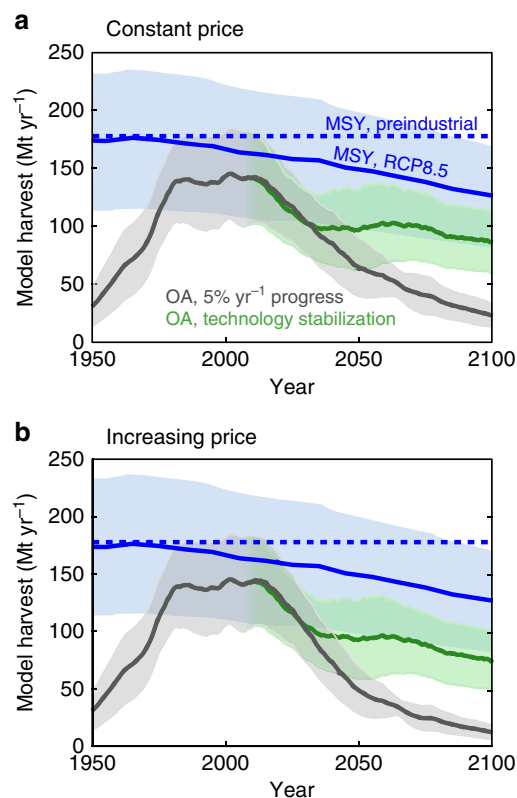


Figure 5 | Future ensemble projections of global harvest under idealized scenarios. In each panel, four different idealized scenarios illustrate a range of possible long-term outcomes, reflecting different roles of technological progress, fisheries management, climate change and market conditions. Black lines show OA simulations, representing an absence of management, with steady 5% per year technological progress. Green ‘technology stabilization’ OA simulations undergo a gradual decrease in technological progress from 5% per year in 2006 to zero by 2036, after which the technology is held constant. The global MSY that could be achieved given perfect management aimed at maximizing harvest is shown in blue. For the OA and MSY RCP8.5 scenarios, the 1 s.d. range of the five ensemble members is shown by shaded envelope. (a) Simulations with constant future price, (b) simulations with linearly increasing price from $\sim 1\$ \text{ kg}^{-1}$ in 2006 to $\sim 3\$ \text{ kg}^{-1}$ in 2100. All OA simulations, as well as the MSY RCP8.5 simulation, use the IPSL Earth System model climate change projection, while the preindustrial MSY is plotted as a constant value, calculated from the mean of the period 1850–1900 in the IPSL historical simulation.

Nonetheless, given the large number of technological innovations that took place over the 20th century, from monofilament lines, power blocks and new hook designs³⁷, to sonar, radar and satellite communications, it is plausible that the overall aggregate progress—integrated among industrial fisheries of the world—may have been relatively smooth.

The impact of technological progress is achieved in the model by two interdependent pathways: fish become easier to catch for a given nominal effort and fish biomass, increasing effective effort, which in turn makes fishing more profitable, thereby increasing the nominal effort as long as the ecosystem is capable of sustaining the harvest. The fact that, over a 50-year period, a 5% per year rate of technological progress would have increased catchability by an order of magnitude explains its dominance over the relatively small historical fluctuations in the ex-vessel price and the cost of fishing.

Our idealized future simulations suggest that, over the 21st century, continuing technological improvements would cause

global harvest to decrease under OA. This reversal of the 20th century trend would be exacerbated by any market dynamics that raise prices. These simulated future decreases, which lead to a growing divergence between OA and MSY over time (Fig. 5), suggest that the global impact of effective regulation will become more important in future as technology improves: whereas in 2015, the simulated MSY harvest is only ~15% greater and ~\$20 billion per year more profitable than the global OA harvest, in 2100 (given 5% per year progress and increasing prices) the MSY harvest is more than ten-fold greater and hundreds of billions per year more profitable than the OA harvest. Although this may be of only theoretical interest for fisheries where effective regulatory regimes are well-established, it could have serious food security implications for the numerous fisheries in which regulations remain ineffective. The model suggests that, if perfectly managed, the global MSY would be on the order of 25% greater than the OA historical peak under preindustrial climate, and that even with the rapid climate change of the RCP8.5 scenario, the MSY would remain greater than the OA historical peak throughout most of the 21st century. Thus, our model suggests that the global wild capture fishery could continue to provide food, throughout the 21st century, at the same rate (or better) as at the end of the 20th century, but only if effective management can be extended to the fisheries in which it remains weak or absent.

We note that if new fisheries develop for previously unexploited species (such as mesopelagic fish), not included in our model, this could potentially slow the reduction of harvest under OA and raise global MSY. At the same time, our model is generally optimistic, in that it does not resolve habitat destruction by intensive trawling³⁸, the takeover of ecosystems by non-commercial species³⁹, trophic cascades⁴⁰, alternative stable states⁴¹, ocean acidification and deoxygenation, or the development of overcapacity due to subsidies⁶, all of which would benefit from further study. The urgent need for improved fisheries management at the global scale is widely recognized, given the existing level of fishing effort¹⁹ and growing pressure from climate change^{42,43}. Our results amplify these concerns by showing that, whereas progress in fishing technology contributed to massive gains in fish harvest during the 20th century at the global scale, its influence on catchability would be expected to only reduce harvest in the 21st century unless met with a global expansion of effective fisheries management.

The model presented here takes a highly simplified approach to the wild capture fishery, as required to remain tractable at the global scale and over long timescales. But despite its simplicity, the comprehensive treatment of critical elements, including spatially and temporally resolved interactions of humans with the ecosystem, allow it to identify the relative importance of general mechanisms that are difficult to discern among the multiplicity of factors typically considered on shorter timescales. Similar approaches may help to better understand the long-term dynamics of other coupled human-Earth systems.

Methods

Model overview. At the foundation of the model is energy production by phytoplankton, which is transferred to multiple fish size-spectra according to an efficiency that depends on gross ecosystem metabolic rates^{16,44,45}. The fish spectra are defined as representing the entire range of finfish and invertebrates with individual mass greater than 10 g, commercially harvested before 2006. The spectra resolve basic life-history characteristics, including temperature-dependent growth, mortality and density-dependent recruitment. By including all commercial species within the spectra, we implicitly account for species range shifts^{46,47}, evolution⁴⁸, and changes in targeted species, all of which have been significant historically and could play important roles in the future.

An economic model, coupled directly to the fish spectra at the grid scale, predicts fishing effort as a function of local profit, assuming open access to the available fish, following the classic work of ref. 49. Fishing effort in each grid cell

changes over time according to the difference between local revenues and costs, at a rate determined by the fleet adjustment timescale. The effectiveness of fishing effort at catching the locally available biomass is determined by a catchability parameter that encapsulates both embodied and disembodied technology. Although fisheries are not strictly open access, and approximately one third of fisheries currently has some form of reasonably effective management¹⁹, the absence of effective management from most of the world's fisheries throughout the 20th century makes it a good approximation at the global scale during the historical period^{21,22} as well as an illustrative example to consider the importance of management in future. The approximate global Maximum Sustainable Yield (MSY) is calculated by conducting transient simulations in which catchability is increased slowly, and summing the maximum harvest obtained in each grid cell. A more complete description of the model is given in 'Model description' in Supplementary Methods.

Parameter selection. We calibrate the most important 13 model parameters through a Monte Carlo method and comparison with observationally estimated fish catches and stock assessments at the LME scale ('Parameter optimization' in Supplementary Methods). Because the LMEs span a very broad range of temperature and primary production, this strategy ensures a robust calibration to both these important variables. For the simulations shown here, we use an ensemble of five optimized models that span the uncertain parameter space as widely as possible, while producing a reasonably accurate simulation.

Model forcing and simulations. The model is forced with ocean temperature and net primary production, either from satellite-based observational estimates, or from the Institut Pierre Simon Laplace (IPSL) global climate model⁵⁰, using the historical hindcast followed by the Representative Concentration Pathway (RCP) 8.5 scenario. The factors at play during the historical transient, according to the model framework, include the increase of catchability due to technology^{24,26}, and an observational estimate of the global average ex-vessel fish price⁵¹, which has varied remarkably little ('Ex-vessel Price variations' in the Supplementary Methods). Given that there is no currently available estimate of historical variations in cost per unit effort, we roughly approximate its potential role using its relationship with observed price, effort and harvest under open-access, and making a steady-state assumption ('Historical global average cost per unit effort' in Supplementary Methods).

For the future projections, the OA model is integrated under four idealized scenarios, two of which assume a continuation of the same 5% per year exponential increase in fishing technology, while the other two simulate a gradual decrease in the rate of progress after 2006, reaching stabilized-technology after 2036. Given that technological progress is clearly continuing through advances such as improved fish tracking, the deployment of fish aggregating devices, and the increasing mechanization of fleets in developing nations, the technology-stabilization scenarios are included as baselines from which to estimate the long-term importance of future technological progress, rather than representing realistic future outcomes. For each of the technological scenarios, we address uncertainty in future market conditions by changing the ex-vessel price. Because the price of fish depends on the demand for fish products, which is difficult to predict given its dependence on societal preferences, available substitutes, and distribution networks⁵², we apply two end-member scenarios for ex-vessel price: linearly increasing, and constant. These represent the outcomes that might come from a larger population and/or a greater preference for seafood (increasing price), or a ready availability of substitutes from terrestrial food production (constant price), and bracket a wide range of intermediate possibilities.

Code availability. The model code was written in MATLAB version R2012a. The zero-dimensional version of the model (that is, for a single patch of ocean), which includes the model run script, required functions, and forcing data, is available for download at <http://dx.doi.org/10.5281/zenodo.27700> (ref. 53).

Data availability. The model output and observational data are available from the authors on request.

References

1. Pauly, D. & Zeller, D. Catch reconstructions reveal that global marine fisheries catches are higher than reported and declining. *Nat. Commun.* **7**, 10244 (2016).
2. Watson, R. A. *et al.* Global marine yield halved as fishing intensity redoubles. *Fish. Fish.* **14**, 493–503 (2013).
3. Hilborn, R. *et al.* State of the world's fisheries. *Ann. Rev. Environ. Resources* **28**, 359–399 (2003).
4. Worm, B. & Branch, T. A. The future of fish. *Trends Ecol. Evol.* **27**, 594–599 (2012).
5. Willman, R., Kelleher, K., Arnason, R. & Franz, N. *The Sunken Billions: the Economic Justification for Fisheries Reform* (IBRD/FAO, 2009).
6. Sumaila, U. R. *et al.* A bottom-up re-estimation of global fisheries subsidies. *J. Bioecon.* **12**, 201–225 (2010).
7. Squires, D. & Vestergaard, N. Technical change in fisheries. *Mar. Policy* **42**, 286–292 (2013).
8. Brander, K. M. Global fish production and climate change. *Proc. Natl Acad. Sci.* **104**, 19709–19714 (2007).

9. Cheung, W. W. *et al.* Large-scale redistribution of maximum fisheries catch potential in the global ocean under climate change. *Glob. Change Biol.* **16**, 24–35 (2010).
10. Quaas, M. F., Reusch, T. B., Schmidt, J. O., Tahvonen, O. & Voss, R. It is the economy, stupid! Projecting the fate of fish populations using ecological-economic modeling. *Glob. Change Biol.* **22**, 264–270 (2016).
11. Carozza, D. A., Bianchi, D. & Galbraith, E. D. The ecological module of BOATS-1.0: a bioenergetically constrained model of marine upper trophic levels suitable for studies of fisheries and ocean biogeochemistry. *Geosci. Model Dev.* **9**, 1545–1565 (2016).
12. Carozza, D. A., Bianchi, D. & Galbraith, E. D. Formulation, general features and global calibration of a bioenergetically-constrained fishery model. *PLoS ONE* **12**, e0169763 (2017).
13. Fulton, E. A. Approaches to end-to-end ecosystem models. *J. Mar. Syst.* **81**, 171–183 (2010).
14. Barange, M. *et al.* Impacts of climate change on marine ecosystem production in societies dependent on fisheries. *Nat. Clim. Change* **4**, 211–216 (2014).
15. Christensen, V. *et al.* The global ocean is an ecosystem: simulating marine life and fisheries. *Glob. Ecol. Biogeogr.* **24**, 507–517 (2015).
16. Jennings, S. *et al.* Global-scale predictions of community and ecosystem properties from simple ecological theory. *Proc. R. Soc. B* **275**, 1375–1383 (2008).
17. Andersen, K. H., Jacobsen, N. S. & Farnsworth, K. D. The theoretical foundations for size spectrum models of fish communities. *Can. J. Fish Aquat. Sci.* **73**, 575–588 (2016).
18. Branch, T. A. *et al.* Fleet dynamics and fishermen behavior: lessons for fisheries managers. *Can. J. Fish Aquat. Sci.* **63**, 1647–1668 (2006).
19. Costello, C. *et al.* Global fishery prospects under contrasting management regimes. *Proc. Natl Acad. Sci.* **113**, 5125–5129 (2016).
20. Larkin, P. A. An epitaph for the concept of maximum sustained yield. *Trans. Am. Fish. Soc.* **106**, 1–11 (1977).
21. Mora, C. *et al.* Management effectiveness of the world's marine fisheries. *PLoS Biol.* **7**, e1000131 (2009).
22. Costello, C., Lynham, J., Lester, S. E. & Gaines, S. D. Economic incentives and global fisheries sustainability. *Ann. Rev. Resource Econ.* **2**, 299–318 (2010).
23. Stott, P. A. *et al.* External control of 20th century temperature by natural and anthropogenic forcings. *Science* **290**, 2133–2137 (2000).
24. Squires, D. & Vestergaard, N. Technical change and the commons. *Rev. Econ. Stat.* **95**, 1769–1787 (2013).
25. Wilberg, M. J., Thorson, J. T., Linton, B. C. & Berkson, J. Incorporating time-varying catchability into population dynamic stock assessment models. *Rev. Fish. Sci.* **18**, 7–24 (2009).
26. Pauly, D. & Palomares, M. *An empirical equation to predict annual increases in fishing efficiency.* Working Paper Series, Working Paper #2010-07 (Fisheries Centre, The University of British Columbia, 2010).
27. Tidd, A. N., Reid, C., Pilling, G. M. & Harley, S. J. Estimating productivity, technical and efficiency changes in the Western Pacific purse-seine fleets. *ICES J. Mar. Sci.: J. Conseil.* **73**, 1226–1234 (2016).
28. Mullon, C., Fréon, P. & Cury, P. The dynamics of collapse in world fisheries. *Fish. Fish.* **6**, 111–120 (2005).
29. Branch, T. A., Jensen, O. P., Ricard, D., Ye, Y. & Hilborn, R. Contrasting global trends in marine fishery status obtained from catches and from stock assessments. *Conserv. Biol.* **25**, 777–786 (2011).
30. Villasante, S. & Sumaila, U. R. Estimating the effects of technological efficiency on the European fishing fleet. *Mar. Policy* **34**, 720–722 (2010).
31. Jackson, J. B. *et al.* Historical overfishing and the recent collapse of coastal ecosystems. *Science* **293**, 629–637 (2001).
32. Swartz, W., Sala, E., Tracey, S., Watson, R. & Pauly, D. The spatial expansion and ecological footprint of fisheries (1950 to Present). *PLoS ONE* **5**, e15143 (2010).
33. Watson, R. A. & Morato, T. Fishing down the deep: accounting for within-species changes in depth of fishing. *Fish. Res.* **140**, 63–65 (2013).
34. Cheung, W. W. *et al.* Building confidence in projections of the responses of living marine resources to climate change. *ICES J. Mar. Sci.: J. Conseil.* **73**, 1283–1296 (2016).
35. Cushing, D. Dependence of recruitment on parent stock. *J. Fish. Board Can.* **30**, 1965–1976 (1973).
36. Myers, R. A. Stock and recruitment: generalizations about maximum reproductive rate, density dependence, and variability using meta-analytic approaches. *ICES J. Mar. Sci.: J. Conseil.* **58**, 937–951 (2001).
37. Eigaard, O. R., Thomsen, B., Hovgaard, H., Nielsen, A. & Rijnsdorp, A. D. Fishing power increases from technological development in the Faroe Islands longline fishery. *Can. J. Fish. Aquat. Sci.* **68**, 1970–1982 (2011).
38. Pusceddu, A. *et al.* Chronic and intensive bottom trawling impairs deep-sea biodiversity and ecosystem functioning. *Proc. Natl Acad. Sci.* **111**, 8861–8866 (2014).
39. Robinson, K. L. *et al.* Jellyfish, forage fish, and the world's major fisheries. *Oceanography* **27**, 104–115 (2014).
40. Andersen, K. H. & Pedersen, M. Damped trophic cascades driven by fishing in model marine ecosystems. *Proc. R. Soc. B* **277**, 795–802 (2009).
41. De Roos, A. M., Boukal, D. S. & Persson, L. Evolutionary regime shifts in age and size at maturation of exploited fish stocks. *Proc. R. Soc. B* **273**, 1873–1880 (2006).
42. Beddington, J. R., Agnew, D. J. & Clark, C. W. Current problems in the management of marine fisheries. *Science* **316**, 1713–1716 (2007).
43. Worm, B. *et al.* Rebuilding global fisheries. *Science* **325**, 578–585 (2009).
44. Brown, J. H., Gillooly, J. F., Allen, A. P., Savage, V. M. & West, G. B. Toward a metabolic theory of ecology. *Ecology* **85**, 1771–1789 (2004).
45. Kooijman, S. A. L. M. *Dynamic Energy Budget Theory for Metabolic Organisation* (Cambridge University Press, 2009).
46. Perry, A. L., Low, P. J., Ellis, J. R. & Reynolds, J. D. Climate change and distribution shifts in marine fishes. *Science* **308**, 1912–1915 (2005).
47. Pinsky, M. L., Worm, B., Fogarty, M. J., Sarmiento, J. L. & Levin, S. A. Marine taxa track local climate velocities. *Science* **341**, 1239–1242 (2013).
48. Kuparinen, A. & Merilä, J. Detecting and managing fisheries-induced evolution. *Trends Ecol. Evol.* **22**, 652–659 (2007).
49. Gordon, H. S. The economic theory of a common-property resource: the fishery. *J. Polit. Econ.* **62**, 124–142 (1954).
50. Dufresne, J.-L. *et al.* Climate change projections using the IPSL-CM5 Earth system model: from CMIP3 to CMIP5. *Clim. Dyn.* **40**, 2123–2165 (2013).
51. Sumaila, U. R., Marsden, A. D., Watson, R. & Pauly, D. A global ex-vessel fish price database: construction and applications. *J. Bioecon.* **9**, 39–51 (2007).
52. Mullon, C. *et al.* Exploring future scenarios for the global supply chain of tuna. *Deep Sea Research Part II: Topical Studies in Oceanography* (in the press).
53. Carozza, D. A., Bianchi, D. & Galbraith, E. D. 0-D Bioeconomic Marine Trophic Size-spectrum (BOATS) model (review version). doi:10.5281/zenodo.27700 (2015).

Acknowledgements

We thank the Canadian Foundation for Innovation (CFI) for providing computing infrastructure, and the Marine Environmental Prediction and Response (MEOPAR) Network Centre of Excellence and Canadian Foundation for Advanced Research (CIFAR) for funding support. EDG acknowledges financial support from the Spanish Ministry of Economy and Competitiveness, through the María de Maeztu Programme for Centres/Units of Excellence in R&D (MDM-2015-0552). This project has received funding from the European Research Council (ERC) under the European Union's Horizon 2020 research and innovation programme (grant agreement No 682602, BIGSEA). D.B. acknowledges financial support from a Faculty Research Grant from University of California Los Angeles.

Author contributions

E.D.G., D.A.C. and D.B. designed the study. D.A.C. and D.B. wrote the model code. D.A.C. and D.B. performed the model simulations. E.D.G., D.A.C. and D.B. contributed to the analysis. E.D.G. wrote the paper with contributions from D.A.C. and D.B.

Additional information

Supplementary Information accompanies this paper at <http://www.nature.com/naturecommunications>

Competing interests: The authors declare no competing financial interests.

Reprints and permission information is available online at <http://npng.nature.com/reprintsandpermissions/>

How to cite this article: Galbraith, E. D. *et al.* A coupled human-Earth model perspective on long-term trends in the global marine fishery. *Nat. Commun.* **8**, 14884 doi: 10.1038/ncomms14884 (2017).

Publisher's note: Springer Nature remains neutral with regard to jurisdictional claims in published maps and institutional affiliations.



This work is licensed under a Creative Commons Attribution 4.0 International License. The images or other third party material in this article are included in the article's Creative Commons license, unless indicated otherwise in the credit line; if the material is not included under the Creative Commons license, users will need to obtain permission from the license holder to reproduce the material. To view a copy of this license, visit <http://creativecommons.org/licenses/by/4.0/>

© The Author(s) 2017

Supplementary Methods

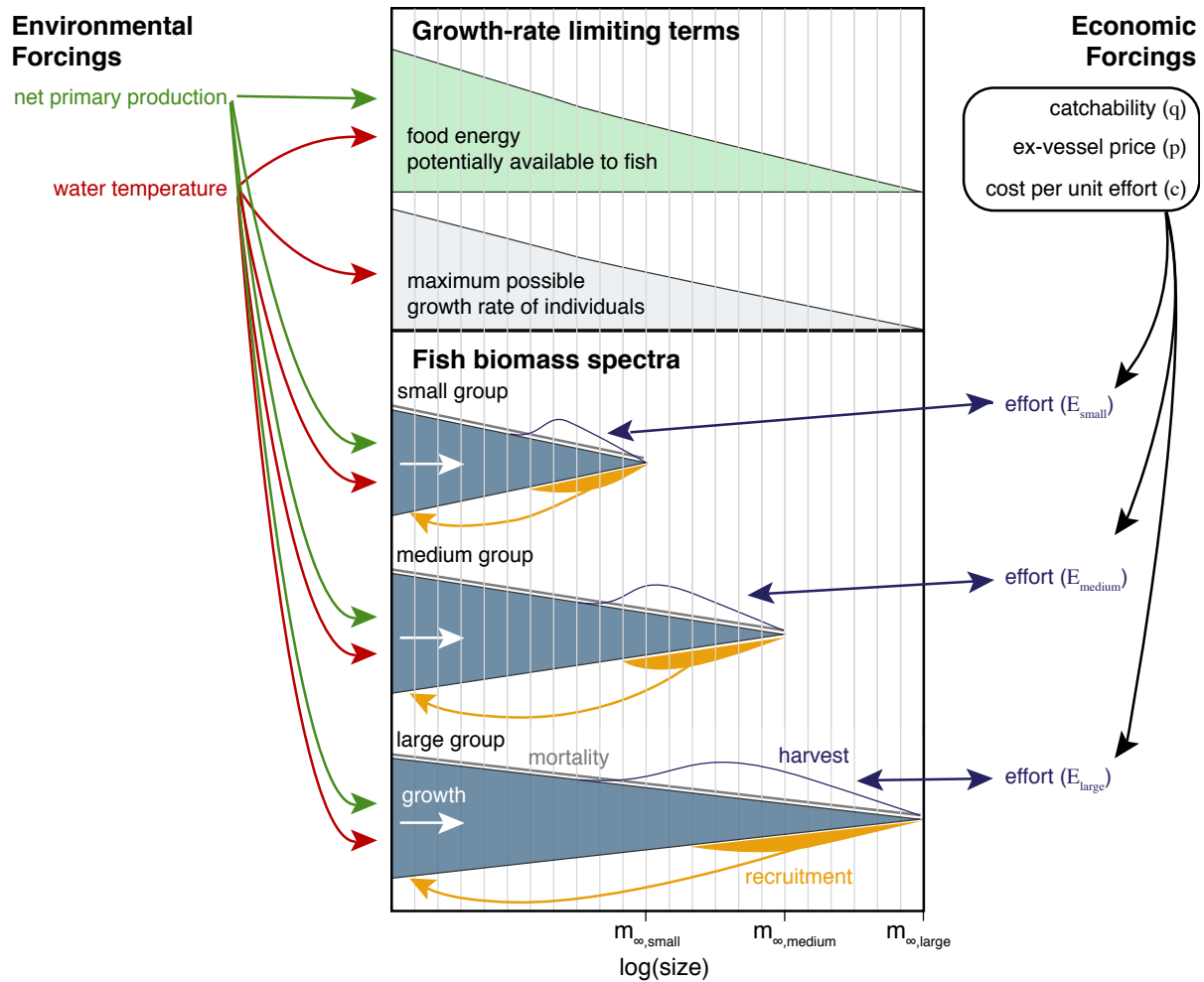
Model description

The ecosystem component of the BiOeconomic mArine Trophic Size-spectrum (BOATS) model takes a macroecological approach, founded on a well-developed body of theory and empirical parameterizations that have been shown to explain many aspects of organisms as a function of size and body temperature. The model is described here briefly; the reader is referred to refs. 1 and 2 for a detailed description.

The configuration of BOATS used here simulates all commercial species as three aggregate size spectra ($k=1:3$), that differ only in their maximum sizes, chosen to correspond to the groups in the Sea Around Us Project (SAUP) database³. These groups are not intended to represent the entire marine ecosystem, but rather the sum of all species that have been commercially harvested (and are therefore accounted for in harvest records, which are used to constrain the model). The underlying philosophy of the model is that, although these very diverse species differ widely in their biological strategies, all are competing for food energy ultimately provided by the fixation of organic carbon through photosynthesis (which has been shown to limit fish harvests, ref. 4), while inhabiting the same environment, which therefore makes them subject to the same metabolic constraints. The constraints we apply in the model are the impacts of water temperature on growth, mortality, and phytoplankton size, and the net primary production. Although this biologically 'coarse-grained' approach precludes resolution of species-level dynamics, it is solidly-founded in bioenergetic principles, and is well-suited to the global view of the entire ecosystem on long timescales, given that it is likely to be relatively robust under any

changes in the distribution, abundance or evolution of commercial species. Supplementary

Figure 1 provides a schematic overview of the model structure.



Supplementary Figure 1. Schematic overview of the BOATS model. The red, green, and black arrows indicate dependencies of model components on external forcings. The top panel indicates the energetic limits of growth as a function of fish size, while the bottom panel illustrates the three size spectra of fish groups, their internal dynamics, and link to economics via harvest and the interactive effort.

Each horizontal grid cell represents the vertically-integrated population of potentially-commercial organisms within that grid cell. The growth of ‘fish’, including finfish and invertebrates, within each spectrum is given by the McKendrick-von Foerster equation,

$$\frac{\partial}{\partial t} f_k = -\frac{\partial}{\partial m} \gamma_k f_k + \frac{\gamma_k f_k}{m} - \Lambda_k f_k \quad (1)$$

where m is a mass element, t is time, f_k is the biomass spectrum per unit area of group k , and Λ_k is the natural mortality rate. The growth rate, γ , for an individual of mass m , is limited by the energy available from photosynthesis in the grid cell, π , which, following ref. 5, is calculated as:

$$\pi = \frac{\Pi}{m} \left(\frac{m}{m_\psi} \right)^{\tau-1} \quad (2)$$

where Π_ψ is the local net photosynthesis, τ is a trophic scaling exponent depending on the average trophic efficiency and predator to prey mass ratio⁵ that indicates how efficiently photosynthetic energy is transferred through the food web, and m_ψ is the geometric-mean size of phytoplankton cells. Each fish group can potentially access an equal fraction ϕ_k of the total primary production energy, representing an exclusive ecological niche. In addition, the growth rate of individuals is limited by a temperature- and size-dependent maximum growth rate,

$$\gamma_{VB} = Am^b - k_a m \quad (3)$$

where A and k_a are temperature-dependent, and b is a constant. This limit represents the biological maximum growth rate when food is not limiting. Thus, the total energy available for growth is

$$\xi_{I,k} = \min \left[\frac{\phi_k \pi m}{f_k}, \gamma_{VB} \right] \quad (4)$$

This energy is then partitioned between somatic growth and reproduction as a function of mass relative to asymptotic mass, following Andersen and Beyer⁶.

The bottom boundary condition of each size spectrum is given by a modified Beverton-Holt⁷ recruitment relationship that depends on integrated spawner biomass and reproduction rate within the spectrum, the water temperature, and on the availability of food, consistent with observations⁸. Although predicting the recruitment of an individual species in any given year has

proven a vexing problem⁹, our model aims for a much more modest goal, which is to predict the total recruitment of all species, classified only by their asymptotic size. Where the biomass production of commercial species is limited by growth rates or egg production, the excess photosynthetic energy is assumed to supply non-commercial species (such as unharvested zooplankton, jellyfish and benthic invertebrates).

The Open Access (OA) economic model is a spatially- and temporally-resolved implementation of the Gordon-Schaefer model^{10,11}. Fish harvest of group k , (H_k) is determined in each grid cell, during each time step, as

$$H_k = q E_k \sigma_k f_k \quad (5)$$

where E_k is the nominal fishing effort applied to the group, σ_k is a function representing the size-selectivity of fishing gear on group k , and q is a catchability parameter that represents the effectiveness of fishing technology in catching the selectable fish biomass. Because the model resolves life history through the size spectrum, the size-selectivity of fishing gear is an important determinant of the impacts of harvest mortality^{12,13}. Although different gear types have different size selectivities, it has been shown that most are sigmoidal, with low selectivity for juveniles, transitioning to nearly complete selectivity across a threshold size^{14,15}. We therefore define the size-selectivity function as

$$\sigma_k = \left[1 + \left(\frac{m}{m_{T,k}} \right)^{-c_\sigma / \delta_2} \right]^{-1} \quad (6)$$

where the threshold mass $m_{T,k}$ is defined by a fraction of the maturity size, given by a position scaling term e_{mT} , and the parameters c_σ and δ define the shape of the selectivity vs. size.

The fishing effort on each group, E_k , evolves independently in each grid cell over the simulation according to the local average profit, which is the difference between the local revenue (the fish price multiplied by the harvest) and the local cost (the fishing cost multiplied by the effort):

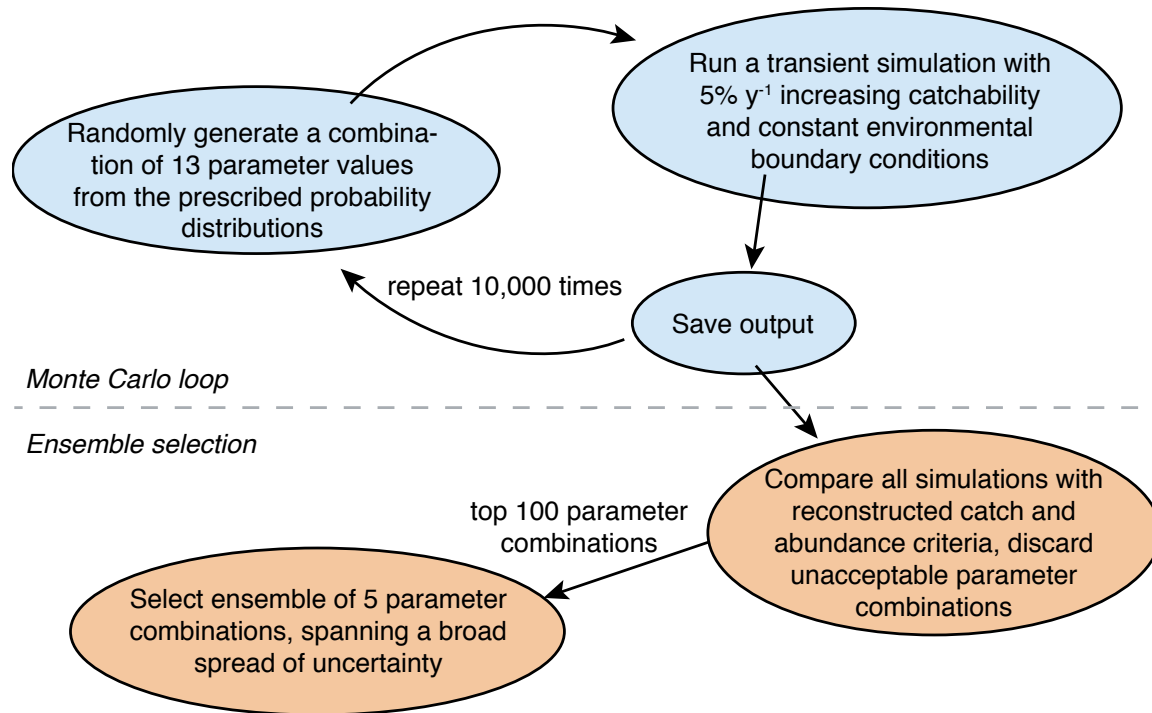
$$\frac{d}{dt} E_k(t) = \frac{\kappa_e [\text{revenue}_k - \text{cost}_k]}{E_k(t)} \quad (7)$$

The fleet adjustment parameter κ_e represents the time required for processes such as gaining access to capital, gear purchase, and organization of labour, and is set so that effort responds on a ten-year timescale to changes in profit. Together, this relatively simple representation captures the dynamics of an open access fishery, leading to zero profit at steady state.

The cost per unit effort is assumed to include investment, repair and maintenance of fishing infrastructure, fuel consumption, and labour cost in bringing the fish to market. As a first approximation, costs are assumed to be spatially uniform, and do not account for distance to port. “Price” is that paid to the fishermen at the point of landing (ex-vessel), and is also spatially uniform, though a temporally-variable price is imposed in some experiments. The possibility of using different prices for different fish sizes was explored, but we failed to identify simple, robust relationships between asymptotic size and price that held across all commercial fish over time. For example, anchovies and shrimp have similar asymptotic sizes, but shrimp tend to be far more valuable per kg. These prices seem to reflect societal preference related to factors such as taste, appearance, convenience or cultural value, rather than fundamental features related to the size, and we therefore consider them difficult to predict.

The model is discretized on a 1-degree grid with a monthly time-step and solved numerically.

Parameter optimization



Supplementary Figure 2. Schematic illustration of the parameter selection.

The model parameters were optimized using a Monte Carlo-based approximate Bayesian computation, schematically illustrated in Supplementary Figure 2. First, 10,000 random combinations of parameter values were chosen from within defined probability distributions (Supplementary Table 1), and for each parameter combination the global model was integrated through a 200 year transient with increasing catchability at 5% y^{-1} , starting from a very low value. Parameter combinations were evaluated by comparing each of the 10,000 simulations to catch data provided by the Sea Around Us Project³ and stock assessment data¹⁶ for 8 LMEs with relatively comprehensive assessments representing >40% of the historically-harvested species (Baltic Sea, Barents Sea, Patagonian Shelf, Benguela Current, North Sea, Okhotsk Sea, Gulf of

Parameter	Name	Sampling distribution	EM1	EM2	EM3	EM4	EM5
$\omega_{a,A}$	Growth activation energy	Normal (0.45, +/- 0.09)	0.31	0.37	0.40	0.43	0.42
$\omega_{a,\lambda}$	Mortality activation energy	Normal (0.45, +/- 0.09)	0.37	0.34	0.64	0.51	0.56
b	Allometric scaling exponent	Uniform (0.61-0.79)	0.67	0.62	0.63	0.69	0.65
A_0	Allometric growth constant	Normal (0.46, +/- 0.5)	0.37	0.40	0.41	0.42	0.40
α	Trophic efficiency	Uniform (0.06-0.20)	0.16	0.16	0.15	0.14	0.18
β	Predator to prey mass ratio	Uniform (675-9330)	7609	1778	8463	7709	8782
k_E	Eppley constant	Normal (0.0631, +/- 0.009)	0.06	0.07	0.05	0.06	0.06
Π^*	Nutrient concentration	Normal (0.37, +/- 0.1)	0.31	0.29	0.20	0.27	0.35
ζ_I	Mortality constant	Normal (0.55, +/- 0.57)	0.27	0.03	0.64	-0.25	0.75
h	Allometric mortality scaling	Normal (0.54, +/- 0.09)	0.6	0.56	0.39	0.51	0.34
s_e	Egg survival fraction	Uniform (0.0001-0.0492)	0.03	0.04	0.01	0.03	0.03
e_{mT}	Selectivity position scaling	Uniform (0.50-1.50)	0.61	1.23	0.54	0.86	0.84
c_σ	Selectivity slope	Uniform (12.0-24.0)	16.7	13.0	20.8	12.4	12.4
		Correlation (Pearson r^2)	0.56	0.51	0.54	0.49	0.56

Supplementary Table 1. Model parameter values varied in Monte Carlo optimization procedure. Parameter values were randomly selected from either a normal distribution (mean, 1 s.d.) or a uniform distribution (min-max) as indicated. The values for each of the five ensemble members (EM) are also given. The last row gives the linear correlation between simulated harvests and the SAUP harvests by LME, for each ensemble member.

Mexico, and East Bering Sea). We then sequentially applied the following four criteria in order to discard 99% of the parameter combinations: 1) the total LME peak harvest was required to fall between 70 and 150 Mt y^{-1} (a very broad range, both to account for uncertainty in the reconstructed harvests and in the allocation of primary production to commercial fish); 2) the global LME peak harvest was required to have medium harvest that was at least 30% of the small harvest and large harvest that was between 10 and 80% of the small harvest; 3) the r^2 between simulated and observed peak LME harvest was required to be at least 0.45 (see discussion below on peak harvests); 4) given that the total assessed harvest:biomass ranged from 0.09 to 0.29 y^{-1} among the 8 thoroughly-assessed LMEs, and considering that none of the

assessments include all potentially commercial species and are therefore quite uncertain, the simulated harvest:biomass ratios of these 8 LMEs were simply required to be less than 0.4 y^{-1} . The application of these four metrics resulted in a total of 100 parameter combinations. Of these, we selected five models that span broad ranges in total global harvest and biomass, in order to represent a large swath of parameter uncertainty (Supplementary Table 1).

Peak harvests as a model calibration target

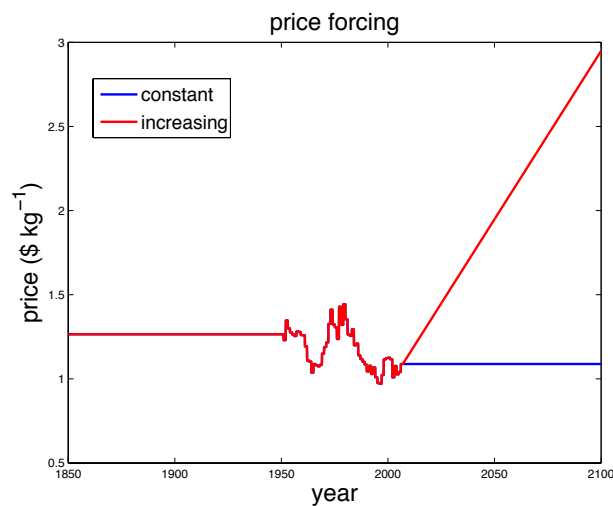
The gradual increase of catchability, q , due to technological progress, produces an inexorable increase of effective effort that causes fish biomass, f , to decrease. Because the harvest (H) is given by $H = q E \sigma f$, (see above), the decrease of f ultimately yields to a decline of harvest, so that a peak in fish harvest occurs at some catchability q_p . The harvest at the q_p peak is therefore a reflection the ability of the ecosystem to produce biomass under a transient increase of fishing pressure^{17,18}, although with caveats. As such, it can be considered an inherent property of an ecosystem that is relatively insensitive to the rate at which effective effort increases, as long as the timescale at which effort increases is longer than the replacement timescale of fish in the ecosystem.

Therefore, where peak harvests can be estimated from observational data, they provide a constraint on the ecosystem's capacity to produce commercial fish, which is a function of ecosystem parameters, and is relatively independent of socio-economic conditions. Effective management could theoretically prevent yields from ever reaching the ecosystem maximum, but given that management was only instigated prior to ecosystem degradation in a few cases (e.g.

the eastern Bering Sea), it is likely that most LME harvest peaks provide a rough indication of ecosystem productivity. Since our model is defined as simulating all commercial species, the total model harvest is directly comparable to the total observed harvest.

We examined the time series of global Large Marine Ecosystems (LMEs) in the SAUP data to define as many peak harvests as possible. Peaks were defined as the average of the 10 highest years of harvest. Model harvest peaks were simulated by forcing the model with continual transient increases of technology, and the corresponding LMEs of the model simulations were compared with observed harvest peaks at 55 LMEs (see 'Parameter optimization'). Although this method is hampered by errors in the observational estimates of fish harvest, it provides a uniquely comprehensive means to calibrate our model over the full global range of marine environments.

Ex-vessel Price variations



Supplementary Figure 3. Ex-vessel price used in historical simulation (red), future constant price (blue) and future increasing price (red).

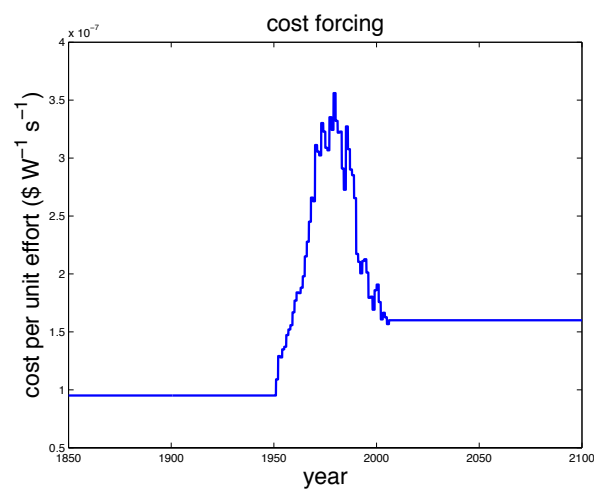
The ex-vessel price is taken from ref. 19 for the period 1950-2006. The price is held constant prior to 1950 at the 1950 value. From 2007-2100, it is either held constant at the 2006 value, or increases linearly at a rate of $2 \text{ \$ kg}^{-1} \text{ century}^{-1}$, similar to the rate of price increase between 1960 and 1975 (see Supplementary Figure 3).

Historical global average cost per unit effort

Although there is a global, observationally-based estimate of cost per unit effort¹⁵, it is only available for a recent time interval, and historical variations over time are not resolved.

Therefore, in order to test the impact that temporally-variable cost per unit effort might have had on the history of global catches, we conducted a pair of sensitivity tests based on a simple line of reasoning.

The open access model employed here simulates changes in effort, E , over time as $dE/dt = (pH - cE)/E$, where p is ex-vessel price and c is cost per unit effort. At steady state, $pH = cE$ and



Supplementary Figure 4. Cost per unit effort, reconstructed as described.

therefore $c=pH/E$. Because p , H and E are all available from observational estimates (see Figure 1 of main text), the average cost per unit effort can be easily calculated, assuming that the fishery is always close to steady state (Supplementary Figure 4).

It is important to recognize that the steady state approximation is incorrect, and this calculation is unlikely to provide an accurate history of the global catch per unit effort. Given that, in reality, the adjustment timescale for E is many years, it cannot respond instantaneously to changes in price, cost and biomass, so that our steady state estimate is likely to provide an exaggerated amplitude of changes in cost over time. For this reason, we do not include it in the simulations other than to test the impact of cost alone. Despite these uncertainties, the reconstruction suggests that globally-averaged historical cost changes did not exceed a factor of 3, and does not suggest a monotonic trend.

Hindcast and projection simulation protocol

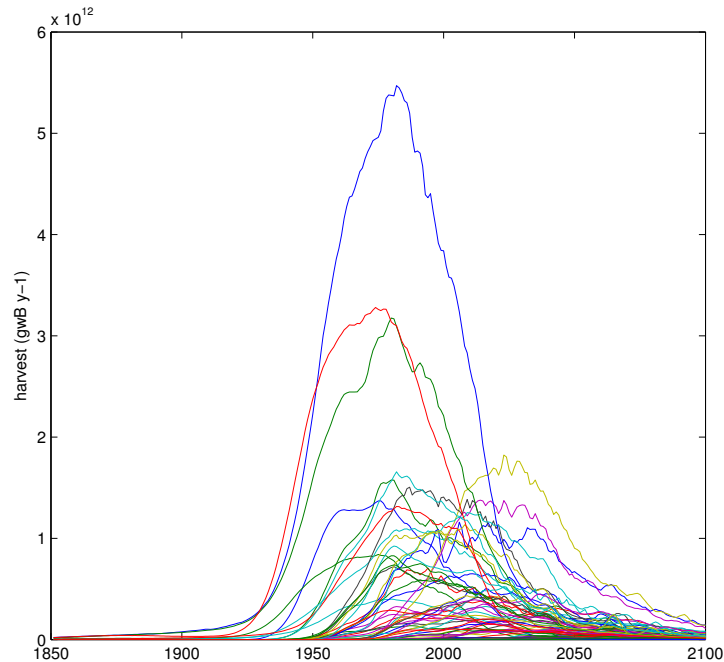
For all ensemble members, we first conducted a spin-up using the steady pre-industrial environmental forcings but without harvest, to represent a global preindustrial fishing state. We then needed to define a relationship between the transient model simulations and historical years, in order to apply the reconstructed ex-vessel price and variable climate simulations, and to compare directly with data. We did this by using the year of global peak harvest as a reference point, identified in the SAUP database as approximately 1995. We then coordinated each ensemble member with this peak year in two steps. First, starting from the preindustrial fishing state, and using the climatological forcing with constant average ex-vessel prices and cost per

unit effort, we imposed a technology increase of $5\% \text{ y}^{-1}$. Then, the model catchability during the peak year was projected backwards using the same $5\% \text{ y}^{-1}$ assumption to give an idealized, low-catchability starting point in calendar year 1850 while ensuring that the peak global harvest will result in the late 1990s; note that we do not expect this procedure to generate a realistic catchability for 1850, it simply serves as a reasonable starting point, to avoid spurious initialization effects. The year of peak global harvest in the full hindcasts is shifted slightly, due to the effects of historically-variable climate and ex-vessel price. Nonetheless, this simple procedure successfully results in peak harvest years between 1995 and 1996 for the five ensemble members, within the uncertainty of the actual peak in the SAUP harvest data.

Global peak in fish harvest

The simulated global peak in fish harvest, shown in Figure 3, is given by the sum of thousands of individual 'fisheries', each operating at a single grid cell, and each of which goes through the classic periods of development, full exploitation, over-exploitation and collapse²⁰.

Supplementary Figure 5 shows the aggregates of these individual grid cell harvests at the LME level for the standard hindcast simulation shown in Figure 3 (for the ensemble member with highest r^2). The transient change of harvest in each LME is dominated by technological progress, with small influences from changes in ex-vessel prices and climate variability, while the differences between LMEs reflect differences in environmental characteristics (NPP and water temperature).



Supplementary Figure 5. Harvest timeseries, aggregated by LME. Each line shows the transient harvest for one LME in the standard hindcast simulation and under the continued 5 % progress with OA (figure 3). Each LME passes through the well-recognized phases of fisheries: a period of development (when harvest is increasing over time), full exploitation (when the harvest reaches a relatively stable peak), over-exploitation (when the harvest starts to decrease) and collapse (when harvest reaches a small fraction of its peak value). The global peak of harvest reflects the sum of these individual ecosystem curves.

Calculation of MSY

Although it has proven to be a problematic term in fisheries science^{21,22}, Maximum Sustainable Yield is nonetheless a useful concept for considering the maximum harvest that could be perpetually extracted from the marine environment assuming no degradation of the ecosystem. We therefore include an estimate of the model's MSY, as constrained by the optimized ecosystem parameters, in order to approximate the total marine food resource that might be obtained under perfect management intended to maximize food production (rather than economic, cultural or other benefit)²³.

The MSY was estimated for each ensemble member by increasing catchability at a very slow rate ($1\% \text{ y}^{-1}$) for 1500 years, after a 200-year equilibration with no harvest. This produces a very smooth, gradual peak of harvest in each grid cell of the model, that closely approximates a succession of steady state harvests each in equilibrium with a different level of catchability. The results were then sampled for the peak harvest achieved in each grid cell, and the results summed in order to give the global peak. In order to calculate the MSY under climate change, the same procedure was followed using a climatology of NPP and temperature obtained from the IPSL transient simulation at 10-year intervals. The result, plotted in Figure 5, interpolates between these 10-year snapshots.

Climate change simulations

In order to test the model sensitivity to climate change, we used output from the Institut Pierre Simon Laplace (IPSL) low-resolution (LR) coupled model. This model was chosen for the fact that its response of global Net Primary Production (NPP) to warming is close to the Coupled Model Intercomparison Project phase 5 (CMIP5) multi-model mean²⁴. The vertically-integrated primary production and shallow subsurface water temperature were used to force the BOATS model ensemble discussed in the main text. In order to clearly show the impact of climate change, we compare a climatological pre-industrial repeating-year (“preindustrial”) with monthly values from the RCP8.5 transient simulation (“RCP8.5”).

The difference in harvest between the preindustrial simulation and the RCP8.5 simulation reflect the sensitivity of the BOATS ecosystem model to the changes of NPP and water temperature

predicted by the IPSL climate-biogeochemical model. This occurs through the impact of water temperature on phytoplankton cell size, organismal growth rates and natural mortality, and the overall energy available to the ecosystem from NPP.

Supplementary References

- 1 Carozza, D. A., Bianchi, D. & Galbraith, E. D. The ecological module of BOATS-1.0: a bioenergetically constrained model of marine upper trophic levels suitable for studies of fisheries and ocean biogeochemistry. *Geosci Model Dev* **9**, 1545-1565 (2016).
- 2 Carozza, D. A., bianchi, D. & Galbraith, E. Reducing parameter uncertainty in a bioenergetically-constrained ecology-economic model of the global fishery. *Plos One* (in press).
- 3 Pauly, D. The Sea Around Us Project: Documenting and communicating global fisheries impacts on marine ecosystems. *AMBIO: a Journal of the Human Environment* **36**, 290-295 (2007).
- 4 Chassot, E. *et al.* Global marine primary production constrains fisheries catches. *Ecology letters* **13**, 495-505 (2010).
- 5 Brown, J. H., Gillooly, J. F., Allen, A. P., Savage, V. M. & West, G. B. Toward a metabolic theory of ecology. *Ecology* **85**, 1771-1789 (2004).
- 6 Andersen, K. H. & Beyer, J. E. Size structure, not metabolic scaling rules, determines fisheries reference points. *Fish and Fisheries* **16**, 1-22 (2015).
- 7 Beverton, R. J. H. & Holt, S. J. *On the Dynamics of Exploited Fish Populations.* (Springer-Science+Business Media, 1957).
- 8 Vert-pre, K. A., Amoroso, R. O., Jensen, O. P. & Hilborn, R. Frequency and intensity of productivity regime shifts in marine fish stocks. *Proceedings of the National Academy of Sciences* **110**, 1779-1784 (2013).
- 9 Houde, E. D. Emerging from Hjort's shadow. *Journal of Northwest Atlantic Fishery Science* **41**, 53-70 (2008).
- 10 Gordon, H. S. The Economic Theory of a Common-Property Resource: The Fishery. *Journal of Political Economy* **62**, 124-142 (1954).
- 11 Schaefer, M. B. Some considerations of population dynamics and economics in relation to the management of the commercial marine fisheries. *Journal of the Fisheries Board of Canada* **14**, 669-681 (1957).
- 12 Jacobsen, N. S., Gislason, H. & Andersen, K. H. The consequences of balanced harvesting of fish communities. *Proceedings of the Royal Society of London B: Biological Sciences* **281**, 20132701 (2014).
- 13 Andersen, K. H. *et al.* Assumptions behind size-based ecosystem models are realistic. *ICES Journal of Marine Science: Journal du Conseil*, fsv211 (2016).
- 14 Millar, R. B. & Fryer, R. J. Estimating the size-selection curves of towed gears, traps, nets and hooks. *Reviews in Fish Biology and Fisheries* **9**, 89-116 (1999).
- 15 Lam, V. W., Sumaila, U. R., Dyck, A., Pauly, D. & Watson, R. Construction and first applications of a global cost of fishing database. *ICES Journal of Marine Science: Journal du Conseil* **68**, 1996-2004 (2011).
- 16 Ricard, D., Minto, C., Jensen, O. P. & Baum, J. K. Examining the knowledge base and status of commercially exploited marine species with the RAM Legacy Stock Assessment Database. *Fish and Fisheries* **13**, 380-398 (2012).
- 17 Srinivasan, U. T., Cheung, W. W., Watson, R. & Sumaila, U. R. Food security implications of global marine catch losses due to overfishing. *Journal of Bioeconomics* **12**, 183-200 (2010).
- 18 Halpern, B. S. *et al.* An index to assess the health and benefits of the global ocean. *Nature* **488**, 615-620 (2012).
- 19 Sumaila, U. R., Marsden, A. D., Watson, R. & Pauly, D. A global ex-vessel fish price database: construction and applications. *Journal of Bioeconomics* **9**, 39-51 (2007).
- 20 Kleisner, K., Zeller, D., Froese, R. & Pauly, D. Using global catch data for inferences on the world's marine fisheries. *Fish and Fisheries* **14**, 293-311 (2013).

- 21 Larkin, P. A. An epitaph for the concept of maximum sustained yield. *Transactions of the American fisheries society* **106**, 1-11 (1977).
- 22 Mace, P. M. A new role for MSY in single-species and ecosystem approaches to fisheries stock assessment and management. *Fish and fisheries* **2**, 2-32 (2001).
- 23 Andersen, K. H., Brander, K. & Ravn-Jonsen, L. Trade-offs between objectives for ecosystem management of fisheries. *Ecological Applications* **25**, 1390-1396 (2015).
- 24 Bopp, L. *et al.* Multiple stressors of ocean ecosystems in the 21st century: projections with CMIP5 models. *Biogeosciences* **10**, 6225-6245 (2013).